JVI Journals.ASM.org

UCLA1, a Synthetic Derivative of a gp120 RNA Aptamer, Inhibits Entry of Human Immunodeficiency Virus Type 1 Subtype C

Hazel T. Mufhandu,[a] Elin S. Gray,[b] Maphuti C. Madiga,[b] Nancy Tumba,[b] Kabamba B. Alexandre,[b] Thandeka Khoza,[a] Constantinos Kurt Wibmer,[b] Penny L. Moore,[b] Lynn Morris,[b,c] and Makobetsa Khati[a,d]

Emerging Health Technologies Platform, Biosciences Unit, CSIR, Pretoria, South Africa[a]; AIDS Virus Research Unit, National Institute for Communicable Diseases, Johannesburg, South Africa[b]; University of the Witwatersrand, Johannesburg, South Africa[c]; and Department of Medicine, Groote Schuur Hospital and University of Cape Town, Cape Town, South Africa[d]

Entry of human immunodeficiency virus type 1 (HIV-1) into cells is mediated by the virion surface envelope (Env) glycoproteins, making it a desirable target for antiretroviral entry inhibitors. We previously isolated a family of gp120 binding RNA aptamers and showed that they neutralized the infectivity of HIV-1. In this study, we assessed the activity of a shortened synthetic derivative of the B40 aptamer, called UCLA1, against a large panel of HIV-1 subtype C viruses. UCLA1 tightly bound to a consensus HIV-1 subtype C gp120 and neutralized isolates of the same subtype with 50% inhibitory concentrations (IC_{50}s) in the nanomolar range. The aptamer had little toxicity in tests with cell lines and primary cells. Furthermore, it exhibited high therapeutic indices, suggesting that it may be effective at very low doses. Mapping of UCLA1 binding sites on gp120 revealed eight amino acid residues that modulated neutralization resistance. This included residues within the coreceptor binding site, at the base of the V3 loop, and in the bridging sheet within the conserved V1/V2 stem-loop of gp120. The aptamer was also shown to have synergistic effects with T20, a gp41 fusion inhibitor, and IgG1b12 (b12), an anti-CD4 binding site monoclonal antibody. These results suggest that UCLA1 may be suitable for development as a potent HIV-1 entry inhibitor.

Human immunodeficiency virus type 1 (HIV-1) binding to T lymphocytes and macrophages is mediated by the glycoprotein gp120, which sequentially interacts with the CD4 receptor and chemokine receptors of the susceptible host cell (3, 4). While gp120 is a heterogeneous molecule with hypervariable loops and extensive glycosylation (27, 28, 52), the CD4 binding site and coreceptor binding site (CoRbs) are both highly conserved (43) and immunogenic (51, 54). Other invariant regions on gp120 include the epitopes defined by the newly isolated broadly neutralizing monoclonal antibodies (MAbs) PG9/16 and PGT127/128 (48, 49), making gp120 a desirable target for agents that block virus entry (35).

Entry inhibitors comprise an array of molecules that target either the virus envelope glycoprotein or host cellular receptors. This includes MAbs, fusion inhibitors, coreceptor antagonists, and small molecule inhibitors (5, 22, 29, 35, 45). Some of these have proven to be effective additions to the reverse transcriptase and protease inhibitors that are presently used to treat HIV-1 infection and are also being considered in prevention science. Artificial nucleic acid ligands called aptamers, which assume a defined three-dimensional structure and generally bind functional sites on their respective targets (15), have been isolated against gp120 and are being developed as potential HIV-1 entry inhibitors (10, 13, 14, 25, 36, 53–56). Aptamers are selected through several rounds of amplification, and they bind a wide range of macromolecules, including those with low immunogenicity or high toxicity (38, 50). They are able to discriminate between targets based on subtle structural changes such as the presence or absence of a methyl or hydroxyl group (38). Due to their high specificity, aptamers can be directed against very defined targets; as a result, they have been applied to a wide range of therapeutics, especially for cancer treatment (54). They can be used to transport inhibitory molecules to specific cells, reducing the off-target effects seen in current treatments (54). Studies have looked at chemically binding or cosynthesizing aptamers and small interfering RNA (siRNA) so that they can be selectively targeted to cells expressing relevant receptors (7, 54). Their small size increases bioavailability and provides access to many biological compartments (24). Furthermore, preparation is fast and simple, allowing for easy scale-up of production.

We have previously isolated 2′-fluoro-substituted RNA aptamers against HIV-1_{BaL} gp120 and shown that they neutralized infectivity of group M and group O HIV-1 clinical isolates in cell-based assays (25). One extensively studied aptamer called B40 was used to produce B40t77, a shortened derivative comprising 77 nucleotides. Subsequently a synthetic, capped derivative of B40t77 called UCLA1 (10) was manufactured by solid-phase synthesis and further shortened and modified to help folding and stability, without compromising its activity (10). The B40 aptamer and its shortened derivatives (B40t77 and UCLA1) have been shown to contact the highly variable exterior surfaces of monomeric and trimeric gp120 and to bind conserved core residues in the CCR5-binding site (10, 13, 14, 23). In one study, using an aptamer related to UCLA1 (aptamer 299.5), mutations within the V3 loop and the bridging sheet (β20) were identified using JR-CSF gp120 monomers (10). In another study, using HIV-1_{BaL} gp120 from viral supernatants (trimeric gp120), mutations in the α1 helix, C2 domain, V3 loop, bridging sheet (β21), and F loop within the C4 domain affected the binding of the B40t77 aptamer (23). While

Received 24 November 2011 **Accepted** 17 February 2012
Published ahead of print 29 February 2012
Address correspondence to Makobetsa Khati, mkhati@csir.co.za.
Supplemental material for this article may be found at http://jvi.asm.org/.

doi:10.1128/JVI.06893-11

some sites were common, discrepancies between these two studies were likely related to the use of different sources of gp120 and different aptamers. In general, both studies suggest that an epitope of the gp120 RNA aptamers overlaps the base of the α1 helix, the CD4-induced binding sites in the bridging sheet (β21 and β20), and the variable loops (F and V3).

Since HIV-1 subtype C dominates the global HIV/AIDS epidemic and is endemic in countries with high HIV-1 prevalence rates such as South Africa (47), where this study was conducted, we assessed the sensitivity of a large panel of subtype C isolates derived from adult and pediatric patients at different stages of HIV-1 infection against UCLA1. We examined its neutralization efficacy and identified the potential binding sites. Furthermore, we evaluated cell viability in the presence of the aptamer and its synergism with other entry inhibitors. Overall, these studies suggest that UCLA1 has properties that make it suitable for further development as a potential HIV-1 entry inhibitor.

MATERIALS AND METHODS

RNA aptamers. The B40t77 and UCLA1 (University of California, Los Angeles) anti-gp120 RNA aptamers were used in this study. B40t77 aptamer (77 nucleotides in length) is a truncated derivative of the full-length B40 RNA aptamer (117 nucleotides in length) previously shown to have anti-HIV inhibitory activity (13, 23, 25). UCLA1 is a derivative of aptamer 299.2, which is a shortened derivative (54 nucleotides in length) of B40t77 (10, 13). The 299.2 aptamer was stabilized by the use of six 2′-O-dimethylallyl ribonucleotides in the short stem 1 together with the insertion of an additional base pair in stem 2 (10). As a result, UCLA1 (also 54 nucleotides in length) is made up of the 299.2 aptamer and chemically modified by the addition of an inverted thymidine at the 3′ end (to block degradation by 3′-exonucleases) and a dimethoxyltrityloxy-$(CH_2)_6$-SS-$(CH_2)_6$-phospho linker at the 5′-end (10). UCLA1 is chemically modified for protection against nucleases and to enhance correct folding and increase its stability for *in vivo* usage (10, 36, 44). An initial batch of UCLA1 was donated for this study by William James, University of Oxford. Subsequent batches were custom synthesized by ATDBio, Ltd., Southampton, United Kingdom.

Cell lines, antibodies, envelope-encoding plasmids, plasma samples, and HIV-1 primary isolates. The TZM-bl cells used for neutralization assay were obtained from the National Institutes of Health (NIH) Reference and Reagent Program. The 293T cells used for transfection were obtained from the American Type Culture Collection (Manassas, VA). The Du151 Env-expressing plasmid (31), Env-pseudotyped viruses, and replication-competent viruses were obtained from the AIDS Virus Research Unit at the National Institute for Communicable Diseases (NICD). The HIV-1 consensus C (ConC) envelope construct was obtained from Feng Gao (26). An HIV-1-positive plasma pool (BB pool) prepared from individual plasma samples as previously described by Li et al. (31), was purchased from the South African National Blood Services in Johannesburg and used as a positive control. IgG1b12 MAb (b12) (NIH Reference and Reagent Program) and T20 fusion inhibitor (Roche, Palo Alto, CA) were obtained from the NICD.

Expression of recombinant HIV-1 consensus C gp120. HIV-1 ConC gp120 was expressed in 293T cells, purified by affinity chromatography using a *Galanthus nivalis* lectin agarose matrix (Sigma-Aldrich, Sweden), and eluted with 1 M methyl-α-D-mannopyranoside (Sigma), as previously described (20). The purity, size, and homogeneity of the protein were assessed using sodium dodecyl sulfate-polyacrylamide gel electrophoresis (SDS-PAGE) and Western blotting as previously described (19). The biological activity of pure proteins was assessed by enzyme-linked immunosorbent assay (ELISA) as previously described (19). Truncated and mutated ConC glycoproteins were generated at the NICD. These included the core gp120 (a mutant that lacks the V1/V2 and V3 loops) (28) and V1/V2-deleted (ΔV1/V2) and V3-deleted (ΔV3) gp120s, as well as gp120 with either the I420R mutation in the CoRbs or the D368R mutation in the CD4 binding site (CD4bs) (32, 40).

Site-directed mutagenesis. Specific amino acid changes in the ConC gp120 were introduced using the QuikChange site-directed mutagenesis kit (Stratagene, La Jolla, CA). The presence of mutations was confirmed by sequence analysis using an ABI Prism BigDye terminator cycle sequencing ready reaction kit (Applied Biosystems, Foster City, CA) and an ABI 3100 automated genetic analyzer. The sequences were assembled and edited using Sequencher (version 4.0) software (Gene Codes, Ann Arbor, MI).

Binding kinetics of RNA aptamers to recombinant HIV-1 consensus C gp120. The BIAcore 3000 surface plasmon resonance (SPR) technology (GE Healthcare) was used to determine the binding kinetics of RNA aptamers to recombinant HIV-1 ConC gp120 with the CM5 biosensor chip by direct amine coupling as described previously (10, 13, 14, 23). The RNA aptamers (UCLA1 and B40t77) were kin injected over the covalently immobilized synthetic HIV-1 ConC gp120. The aptamers were diluted in 1× refolding buffer prior to injection, as previously described (23). Binding kinetics to measure the association and dissociation constants of the aptamers from the protein were measured by kin injecting ½ $\log_{10}$ serial dilutions of the aptamers at a flow rate of 5 μl/min with a 5-min association phase and a 10-min dissociation phase. The BIAcore was also used to determine the binding kinetics of UCLA1 to truncated and mutated HIV-1 ConC gp120 compared to the binding kinetics of the wild-type ConC gp120. The truncated gp120s were the core, ΔV1/V2, and ΔV3 gp120. The core gp120 lacks amino acid residues 128 to 194 (V1/V2 loop) and 298 to 329 (V3 loop), ΔV1/V2 gp120 lacks amino acid residues 128 to 194, and ΔV3 gp120 lacks amino acid residues 298 to 329 (12, 28). The residues are numbered according to HxB2 numbering. The mutated gp120s contained single mutations in the CD4bs (D368R) or CoRbs (I420R). Each experiment was performed at least three times in triplicate using three neighboring flow cells, and the fourth flow cell served as a negative control. The association (K_a) and dissociation (K_d) constants of the resulting data curves were separately fitted to a 1:1 Langmuir binding model and analyzed using the BIAevaluation 4.1 software to obtain the equilibrium dissociation constant (K_D) values. The negative control flow cell and buffer effects were subtracted as a baseline.

Cytotoxicity assay. The cytotoxicity of UCLA1 RNA aptamer was determined by using two cell viability assays. The ATP-based CellTiter-Glo luminescent cell viability assay (Promega) was used as previously described (33). A tetrazolium compound [3-(4,5-dimethylthiazol-2-yl)-5-(3-carboxymethoxyphenyl)-2-(4-sulfophenyl)-2H-tetrazolium, inner salt; MTS]-based CellTiter 96 aqueous cell proliferation assay (Promega) was also used according to the manufacturer's protocol. That is, the dehydrogenase enzymes found in metabolically active cells converts a tetrazolium compound (MTS) into aqueous, soluble formazan which is then quantified by measuring absorbance at 490 nm. The assay was performed in both TZM-bl cells and peripheral blood mononuclear cells (PBMCs). The TZM-bl cells were used at 5×10^5 cells/well in 50 μl Dulbecco's modified Eagle's medium (DMEM) with 5% fetal bovine serum (FBS). The phytohemagglutinin/interleukin-2-stimulated (PHA/IL-2) peripheral blood mononuclear cells (PBMCs) were used at 5×10^4 cells/well in 50 μl RPMI 1640 with 5% FBS. Both cell types were incubated with 500 nM (50 μl) 2-fold serially diluted UCLA1 in triplicate for 72 h at 37°C. The cells used for positive control cultures were treated with etoposide phosphate, an anticancer agent that inhibits topoisomerase II enzyme, which aids in DNA unwinding, thus causing DNA strands to break (39). The positive control cells were incubated with 50 μl of 142 μM etoposide phosphate in triplicate for 72 h at 37°C in 5% CO_2 and 95% humidity. Untreated cell cultures were used as negative controls. The MTS-phenazine methosulafte (PMS) solution (20 μl) was then added to each well and incubated for 4 h at 37°C. To measure the amount of soluble formazan produced by cellular reduction of the MTS, absorbance was recorded at 490 nm using the ELISA plate reader. Titers were calculated as CC_{50} values indicating a 50% reduction in relative light units or in absorbance com-

TABLE 1 Inhibition of HIV-1 subtype C envelope pseudotype viruses by UCLA1 RNA aptamer

Env clone	Subtype	Patient	Stage of infection	Tropism	Accession no.	% inhibition by 50 nM UCLA1[a]	IC_{50} (nM)[b]	TI[c]
HXB2.C8.3	B	Adult	Chronic	X4	AF358142	**98.5 ± 1.73**	0.17	5,882
CAP63.2.00.A9J	C	Adult	Acute	R5	EF203973	**90.8 ± 3.24**	0.14	7,143
ZM233 M.PB6	C	Adult	Acute	R5	DQ388517	**87.8 ± 4.98**	0.04	25,000
CAP210.2.00.E8	C	Adult	Acute	R5	DQ435683	**87.5 ± 6.82**	0.09	11,111
Du156.12	C	Adult	Acute	R5	DQ411852	**86.0 ± 2.37**	0.63	1,587
CAP85.2.00.09J	C	Adult	Acute	R5	EF203985	**84.5 ± 8.50**	0.04	25,000
ZM197.M.PB7	C	Adult	Acute	R5	DQ388515	**83.7 ± 3.14**	0.38	2,632
Consensus C	C	Synthetic		R5	DQ401075	**82.8 ± 6.12**	0.10	10,000
RP1.12	C	Pediatric	Chronic	X4	DQ447271	**81.5 ± 8.66**	0.60	1,667
CAP256.2.00.C7J	C	Adult	Acute	R5	EF203981	**78.8 ± 3.41**	0.16	6,250
CAP45.2.00.G3J	C	Adult	Acute	R5	DQ435682	**77.0 ± 10.88**	0.30	3,333
CAP228.2.00.51J	C	Adult	Acute	R5	EF203968	**76.6 ± 6.06**	0.31	3,226
CAP61.2.00.E11J	C	Adult	Acute	R5	EF203959	**76.5 ± 1.73**	0.38	2,632
ZM214 M.PL15	C	Adult	Acute	R5	DQ388516	**76.0 ± 1.15**	0.23	4,348
SW7.14	C	Adult	Chronic	X4	AF411966	**74.5 ± 4.04**	0.73	1,370
TM3.8	C	Pediatric	Chronic	R5	DQ447268	**74.2 ± 9.71**	0.13	7,692
ZM249 M.PL1	C	Adult	Acute	R5	DQ388514	**74 0.0 ± 1.31**	0.55	1,818
CAP88.2.00.B5J	C	Adult	Acute	R5	EF203972	**73.8 ± 4.37**	0.95	1,053
Du172.17	C	Adult	Acute	R5	DQ411853	**72.3 ± 8.12**	0.60	1,667
CAP239.2.00.F5J	C	Adult	Acute	R5	EF203984	**72.0 ± 8.35**	0.19	5,263
CAP255.2.00.16J	C	Adult	Acute	R5	EF203982	**70.0 ± 0.89**	0.28	3,571
Du422.1	C	Adult	Acute	R5	DQ411854	**69.8 ± 4.96**	0.33	3,030
CAP08.2.00.F6J	C	Adult	Acute	R5	EF203976	**69.7 ± 1.37**	0.95	1,053
CAP206.2.00.8J	C	Adult	Acute	R5	EF203967	**68.2 ± 11.06**	0.66	1,515
CAP248.2.00	C	Adult	Acute	R5	FJ229824	**68.0 ± 3.30**	0.62	1,613
RP6.6	C	Pediatric	Chronic	R5	DQ447269	**67.5 ± 2.78**	0.44	2,273
CAP244.2.00.D3	C	Adult	Acute	R5	DQ435684	**67.0 ± 1.15**	0.44	2,273
RP4.3	C	Pediatric	Chronic	R5	DQ447270	**66.3 ± 6.71**	0.48	2,083
TM7.9	C	Pediatric	Chronic	R5	DQ447267	**63.8 ± 1.58**	0.16	6,250
ZM53 M.PB12	C	Adult	Acute	R5	AY423984	**62.0 ± 4.65**	0.75	1,333
COT9.6	C	Pediatric	Chronic	R5	DQ447272	46.3 ± 2.25	NT	ND
CAP84.2.00.32J	C	Adult	Acute	R5	EF203963	46.0 ± 3.78	NT	ND
ZM109F.PB4	C	Adult	Acute	R5	AY424138	39.7 ± 9.48	NT	ND
Du151.2	C	Adult	Acute	R5	DQ411851	33.0 ± 10.50	NT	ND
Du123.6	C	Adult	Acute	R5	DQ411850	32.3 ± 13.69	NT	ND
COT6.15	C	Pediatric	Chronic	R5	DQ447266	30.0 ± 8.08	NT	ND

[a] Average percentage of inhibition of the respective Env-pseudotyped viruses by the UCLA1 aptamer used at a concentration of 50 nM. Viruses that exhibited more than 50% inhibition (values in boldface) were considered sensitive to neutralization. The average percentage of inhibition ± SD is shown for triplicate data.

[b] IC_{50} is the concentration of the UCLA1 aptamer that inhibited entry of the respective viruses by 50%. Viruses for which titers were not determined (NT) and which exhibited less than 50% inhibition were considered not neutralized.

[c] TI values were obtained by the general formula CC_{50}/IC_{50}. TIs could not be determined (ND) for viruses for which titers were not determined.

pared to the aptamer control after subtracting the background (without aptamer). Thus, CC_{50} is the concentration of the aptamer that would cause cytotoxicity or inhibit cell viability by 50%.

Production of pseudovirus stocks. Env-pseudotyped virus stocks were generated, and the 50% tissue culture infective doses ($TCID_{50}$) were quantified as previously described (17, 19, 34). These were derived from the CAPRISA 002 acute infection study cohort (18), subtype C reference panel (31), pediatric and AIDS patients' isolates (9, 17), and a subtype C consensus sequence clone (ConC) (26). The subtype C pseudoviruses were all R5 strains, except for RP1 and SW7, which were X4 viruses (Table 1). An X4-tropic subtype B pseudovirus, HxB2 reference strain, was also used. A pseudovirus with the vesicular stomatitis virus G (VSV-G) envelope gene was used as the negative control. The mutated ConC gp120 virus stocks were generated, and their $TCID_{50}$s were quantified as previously described (17, 19, 34).

Single-cycle neutralization assay. Neutralization was measured as a reduction in luciferase gene expression after a single-round infection of TZM-bl cells with Env-pseudotyped virus as previously described (17, 34). UCLA1 was tested at a maximum initial concentration of 50 nM and was 3-fold serially diluted in DMEM with 5% FBS without dextran. The positive control BB pool was used at an initial dilution of 1:45. The assay was performed at least three times, in duplicate, for each pseudovirus tested. Titers were calculated as inhibition concentration (IC_{50}) or reciprocal plasma dilution (ID_{50}) values causing 50% reduction of relative light units compared to the virus control (without inhibitor) after subtracting the background (without virus).

Neutralization of primary infectious viruses. Neutralization was measured as a reduction of p24 antigen production of HIV-1 subtype C primary isolates in PHA-stimulated PBMCs as described previously (1, 6). The neutralization assay was performed with 500 $TCID_{50}$s of HIV-1 primary isolate in 3-fold serially diluted UCLA1 at an initial concentration of 100 nM in 40 μl of RPMI 1640 medium supplemented with 5% FBS, 5% interleukin-2 (IL-2), and gentamicin (50 μg/ml) (growth medium). The culture supernatant was collected on days 3, 5, and 7 and replaced with an equal amount of fresh growth medium. For each harvest, the p24 antigen concentration was measured by ELISA using the Vironostika HIV-1 antigen Microelisa system (bioMérieux, Boseind, Netherlands), according to the manufacturer's instructions. The assay was performed at least three

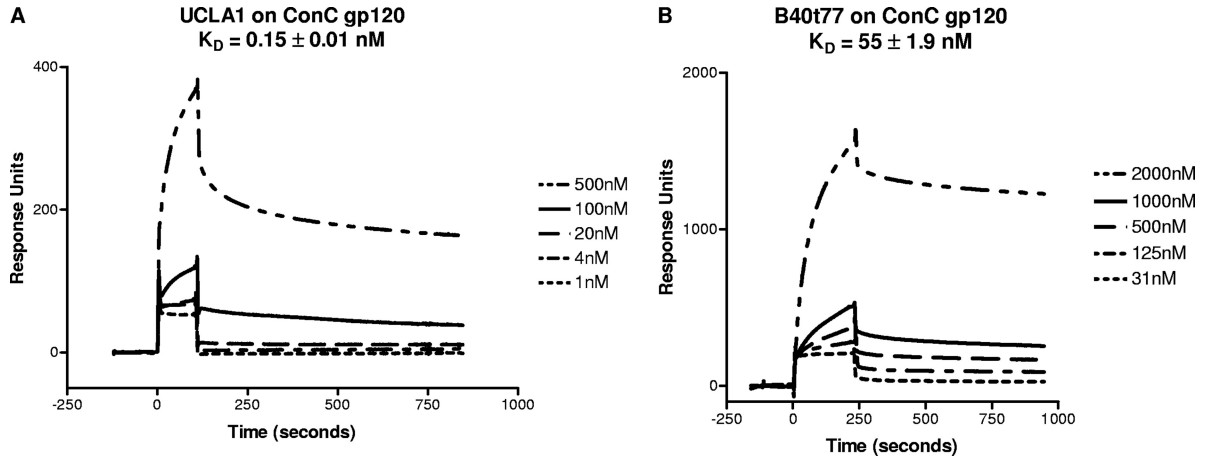

FIG 1 (A) BIAcore sensorgram showing the equilibrium dissociation constant (K_D) of UCLA1 from a synthetic HIV-1 ConC gp120. The aptamer was simultaneously injected over the immobilized gp120 at ½ $\log_{10}$ dilutions with the initial concentration at 500 nM followed by 100 nM, 20 nM, 4 nM, and 1 nM. (B) BIAcore sensorgram showing the K_D of B40t77 aptamer from HIV-1 ConC gp120. The aptamer was simultaneously injected over the immobilized gp120 at 2-fold dilutions with the initial concentration at 2,000 nM, followed by 1000 nM, 500 nM, 125 nM, and 31 nM.

times, in triplicate, for each primary isolate tested. The IC_{80} values were calculated as p24 antigen titers causing 80% reduction of p24 antigen production compared to the virus control (without inhibitor).

Synergy of UCLA1 with other entry inhibitors. UCLA1 was tested for synergism with the CD4bs MAb, b12, and the T20 fusion inhibitor. The single-cycle neutralization assay was used to test a total of 6 Env-pseudotyped viruses with UCLA1-T20 and UCLA1-b12 combinations. The agents were mixed in a fixed ratio that reflected their relative individual potency. The aptamer was used at a maximum initial concentration of 50 nM, while b12 and T20 were used at a maximum initial concentration of 50 μg/ml, equivalent to 312 μM and 11,131 μM, respectively. The assay was performed at least three times in duplicate for each virus tested. The synergy was quantified and expressed as a combination index (CI) using the IC_{50}s (8). Calculation of the CI was based on the Chou-Talalay equation: $CI = (D)_1/(Dx)_1 + (D)_2/(Dx)_2$, in which $(Dx)_1$ and $(Dx)_2$ in the denominators are the concentrations of agent 1 and agent 2 alone that are required to neutralize the HIV-1 subtype C Env pseudovirus, and D_1 and D_2 in the numerators are the concentrations of agent 1 and agent 2 when used in combination that also neutralize the virus. A CI value of less than 1, equal to 1, or more than 1, indicates synergism, an additive effect, and antagonism, respectively (8, 59). A dose reduction index (DRI) was also determined for each combination therapy used. The DRI is a measure of how many fold the dose of each compound in a synergistic combination may be reduced at a given effect level compared with the doses of each compound alone. The DRI was calculated using the Chou-Talalay equation: that is, DRI_1 and DRI_2 are the first and second terms of the CI equation, respectively. Therefore, $DRI_1 = (Dx)_1/(D)_1$ and $DRI_2 = (Dx)_2/(D)_2$ (8, 37, 59).

RESULTS

Binding of RNA aptamers to recombinant HIV-1 consensus C gp120. In order to determine the binding kinetics of B40t77 (unmodified aptamer) and UCLA1 (modified aptamer) to ConC gp120, the protein was immobilized onto a CM5 chip to obtain the dissociation equilibrium constant (K_D) values. A tight binding of the UCLA1 to ConC gp120 was observed with an average K_D of 0.15 nM, a standard deviation (SD) of the mean of 0.01, and a χ^2 value of 1.8 ± 0.7 (Fig. 1A). A χ^2 value of less than 2 demonstrates an acceptable fit of the data to the binding model exhibiting appropriate binding of the aptamer to the gp120 (23). The B40t77 aptamer exhibited higher K_D values than UCLA1, with an average K_D of 55 ± 1.9 nM and a high χ^2 value of 31 ± 5.4 (Fig. 1B). These data established that the modified aptamer had higher binding affinity for gp120 compared to the unmodified aptamer, and thus for all further experiments, we made use of the higher-affinity UCLA1 aptamer.

UCLA1 neutralization of Env-pseudotyped viruses. UCLA1 was tested in the TZM-bl neutralization assay against a panel of *env*-pseudotyped viruses isolated from adult and pediatric patients at different stages of HIV infection. The aptamer inhibited entry of 29 of 35 (83%) subtype C viruses by >50% (range, 62 to 91%), (Table 1). Six viruses showed a reduced sensitivity with <46% neutralization and were considered to be resistant. Of the 29 subtype C viruses neutralized by UCLA1, 27 were R5-tropic and two were X4-tropic strains. The HxB2 (IIIB) virus, which is an X4 subtype B lab-adapted reference strain and generally neutralization sensitive, was almost completely neutralized (99%) by UCLA1 (Table 1).

All viruses' titers were determined against a 3-fold serially diluted UCLA1 starting at 50 nM to calculate IC_{50}s. The IC_{50}s were less than 1.0 nM, with an average of 0.8 ± 0.9 nM for all of the 29 sensitive viruses (Table 1). Representative graphs are shown for 9 sensitive and 3 resistant viruses (see Fig. S1 in the supplemental material). UCLA1 neutralized the sensitive viruses in a dose-dependent manner, while the curves of the 3 resistant viruses did not reach the 50% cutoff, although they were sensitive to the positive control from HIV-infected donors (BB pool) (see Fig. S1). The UCLA1 neutralization curves often exhibited gradual slopes that reached a plateau at less than 100% neutralization, in contrast to curves for the BB pool, which exhibited sharp slopes. Although neutralization curves with similar profiles have been reported previously using MAbs, the mechanism for this is not well understood (21, 41, 49).

Neutralization of HIV-1 primary isolates. To determine the ability of UCLA1 to inhibit HIV-1 subtype C infection of primary cells, neutralization assays were performed using infectious subtype C clinical isolates in PBMCs. Viral infection was measured by p24 ELISA after 5 days of culture. Four of the 6 (67%) primary isolates were neutralized by UCLA1 in a dose-dependent manner

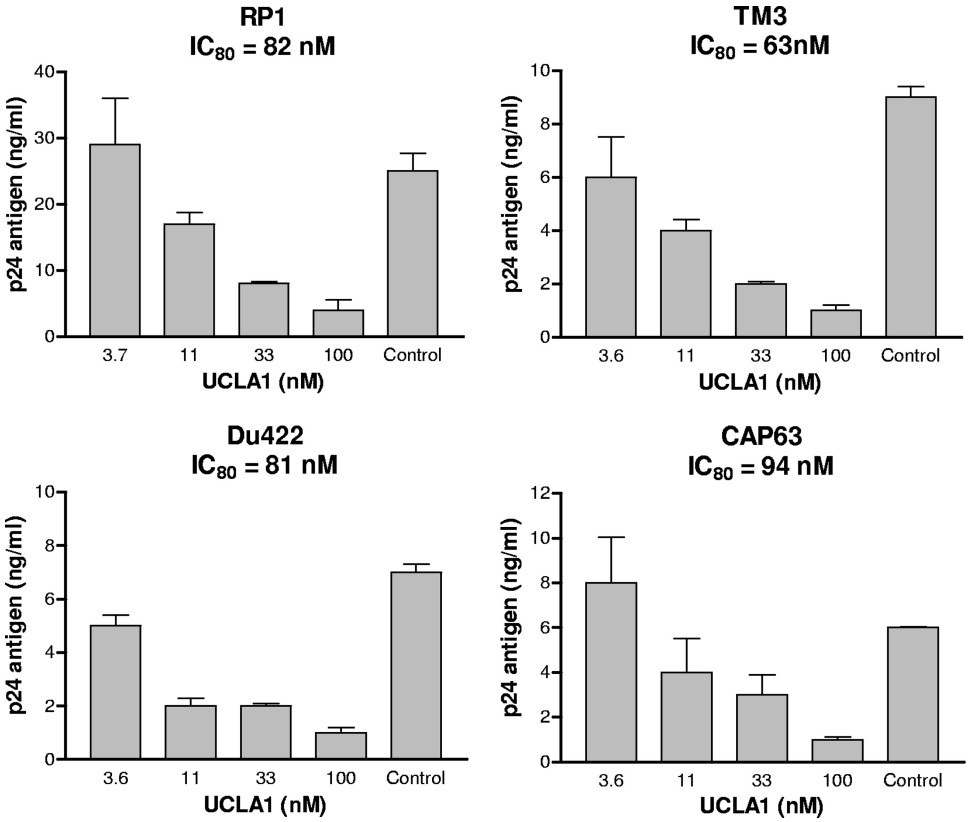

FIG 2 UCLA1 neutralization of HIV-1 subtype C primary isolates in PBMCs. UCLA1 was used at a starting concentration of 100 nM. The IC_{80} values were calculated as p24 antigen titers causing 80% reduction of p24 antigen production compared with the virus control (without UCLA1). The bars represent a dose-dependent inhibition of the p24 antigen by UCLA1. The assay was performed at least three times, in triplicate, for each primary isolate tested.

(Fig. 2). The concentration of the aptamer that inhibited 80% of virus infection (IC_{80}) was within a range of 63 to 94 nM. The 4 included primary viruses isolated from acutely infected adults (Du422 and CAP63) and chronically infected infants (RP1 and TM3), all of which used CCR5, except RP1, which was X4 (Table 1). Two isolates (SW7 and Du156) were not neutralized by UCLA1 in the PBMC assay despite their corresponding cloned envelopes being neutralized in the TZM-bl assay (Table 1). Indeed there was no correlation between the degrees of inhibition for each of the 4 sensitive viruses when the two assays were compared (Table 1 and Fig. 2).

UCLA1 is not cytotoxic and has a wide therapeutic index. The cytotoxicity of UCLA1 was first examined in TZM-bl cells with the ATP-based CellTiter-Glo luminescent cell viability assay. The cells remained 90 to 100% viable after 24 h of incubation with 500 nM UCLA1 (Fig. 3). The aptamer was further tested for cytotoxicity in both PBMCs and TZM-bl cells with the MTS-based CellTiter 96 aqueous cell proliferation assay. The PBMCs exhibited an average viability of 99% ± 0.11%, while the TZM-bl cells had an average viability of 95% ± 0.11%, after 72 h of incubation (Fig. 3). Both cell types were tested with a maximum concentration of 500 nM UCLA1. TZM-bl cells incubated with etoposide phosphate, which was used as a positive control, showed 3% ± 1% viability compared to PBMCs, which showed 36% ± 1% viability.

The estimated therapeutic index (TI) of the aptamer was calculated using the general formula TI = CC_{50}/IC_{50}, for all of the tested viruses. Since 90 to 100% of the cells remained viable after incubation with a maximum concentration of 500 nM UCLA1, we estimated the CC_{50} to be ≥twice the maximum concentration of the aptamer (i.e., 1,000 nM). Thus, the TI was calculated at a standard CC_{50} of 1,000 nM. The average estimated TI of UCLA1 was therefore 5,096 ± 2,285 (range, 25,000 to 1,053) for the 83% neutralized subtype C Env-pseudotype viruses (Table 1).

Mapping aptamer neutralization sites using the ConC Env-pseudovirus. The amino acid residues involved in sensitivity to neutralization were determined using a panel of 19 single site-directed point mutations made in the ConC Env-pseudotyped virus (Table 2). Six of these (K121A, I307A, R419A, K421A, I423A, and A440E) were selected based on published data that implicated these sites in aptamer binding (10, 23). Two additional published residues (R298 and P299) could not be tested due to low virus yields. Five mutations (S365I, S375M, V430A, F468V, and G471E) were included based on sequence alignment of the tested Env-pseudoviruses that were neutralized by the aptamer compared to those that were not neutralized. The remaining 8 mutations (L125A, K305A, R308A, H330Y, N332A, L369P, D474A, and R476A) were selected from available constructs since they were within the CD4bs and CoRbs of gp120. Of the 19 single point mutants tested, 8 conferred resistance to the aptamer in a single-cycle neutralization assay, with all exhibiting IC_{50}s of >10 nM and a range of 10- to 30-fold effect compared to wild-type virus (Fig. 4A and Table 2). A schematic representation of the location of

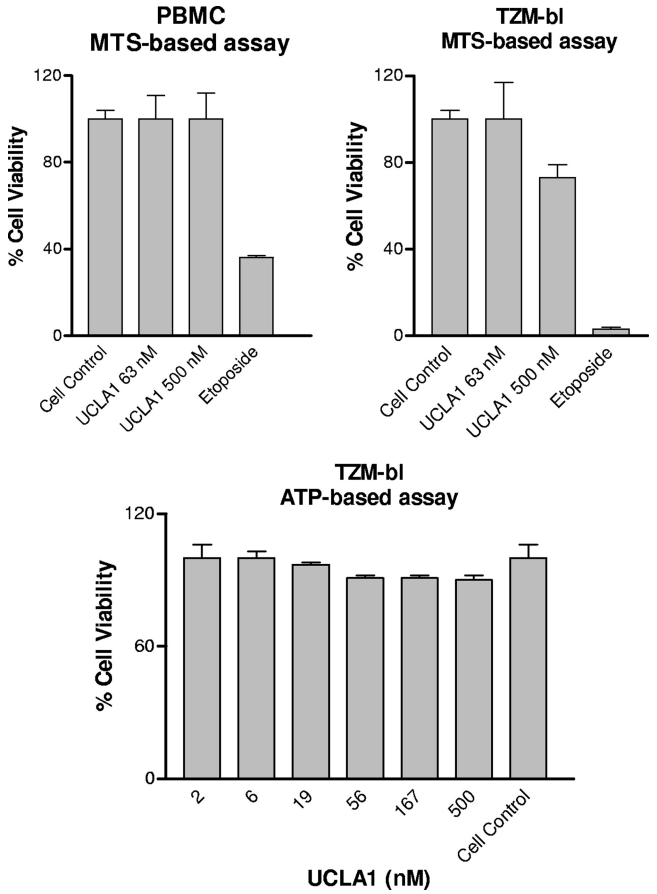

FIG 3 Percentage viability of TZM-bl cells and PBMCs in the presence of various concentrations of UCLA1. Two different assays were used to assess the cytotoxicity of the aptamer. The ATP-based assay was used to test the viability of TZM-bl cells, and the MTS-based assay was used to test the viability of both the TZM-bl cells and PBMCs. Etoposide phosphate was used in the positive control cultures of the MTS-based assay. Untreated cell cultures were used as negative controls. The assays were done three times in triplicate.

these residues on gp120 is shown in Fig. 4B. Overall, the mutations were found within the CoRbs at the base of the V3 loop (K305A, I307A, R308A, and H330Y), in the bridging sheet within the conserved V1/V2 stem-loop of gp120 (K121A and L125A), and within the C4 region (R419A) and the CD4-induced epitope in the C3 region (L369P).

Mapping aptamer binding sites using ConC gp120 proteins. To further explore the dependence of UCLA1 on regions of gp120, we examined the binding kinetics to core gp120 as well as ΔV1/V2 gp120 and ΔV3 gp120. In addition, gp120 proteins containing a single mutation in the CD4bs (D368R) or the CoRbs (I420R) were also tested. The relative K_Ds for each of these proteins are shown in Fig. 5, and the corresponding sensorgrams are shown in Fig. S2 in the supplemental material. For core gp120, the average K_D was 0.7 ± 0.9 nM, which was ~5-fold higher than the K_D of wild-type ConC gp120 (0.15 ± 0.01 nM), confirming the role of variable loops in aptamer binding. Indeed, contributions from both V1/V2 and V3 were evident based on the average K_D values for ΔV1/V2 (0.4 ± 0.1 nM) and ΔV3 (0.5 ± 0.1 nM) gp120s. Interestingly, similar levels were obtained for the I420R and D368R gp120s, sites which could not be tested by neutralization as these viruses are nonfunctional, but which nevertheless confirm the CoRbs and the CD4bs as modulating sites for aptamer binding. While these binding data generally support the neutralization data, it is important to note that assessing epitopes on monomeric gp120 is inherently different from assessing those found on the trimeric complex on the viral membrane. This was evident with Du151, whose pseudotyped virus was not sensitive to UCLA1 (Table 1; see Fig. S1 in the supplemental material), despite its gp120 having a K_D value of 5.8 ± 2.2 nM and a χ^2 value of 3.1 ± 1.2 (see Fig. S3 in the supplemental material).

Sequence analysis of neutralization-resistant viruses. The amino acid sequences of the Env-pseudotype viruses that were not neutralized by UCLA1 were aligned with ConC gp120 and examined for residues shown to confer resistance (see Fig. S4A in the supplemental material). The ZM109 virus that was not neutralized in the TZM-bl assay contained H330Y, which was identified as conferring resistance by ConC point mutational analysis (Fig. 4). COT6, COT9, and Du151 viruses contained K305R/Q, and Du151 also had R419K. Overall, 4 of the 6 viruses that were resistant in the TZM-bl assay had substitutions at residues that were identified as resistance mutations by ConC epitope mapping. Although K305R/Q, H330Y, and R419K had an effect on aptamer binding in these resistant viruses, other viruses that contained the same mutations were sensitive to UCLA1, suggesting context dependence (see Fig. S4A). Reasons for the resistance of the other 2

TABLE 2 Effect of single point mutations on the neutralization of the ConC virus by the UCLA1 aptamer

gp120 region	Binding site	ConC gp120 mutation(s)[a]	Mutant IC_{50} (nM)[b,c]	Fold effect for mutant vs wild type[c,d]
C1	CoR	K121A	**28**	**17**
	CD4	L125A	**40**	**24**
V3		K305A	**41**	**25**
		I307A	**36**	**22**
		R308A	**35**	**21**
	CoR	H330Y	**17**	**10**
		N332A	0.11	0.06
C3	CD4	S365I	6	4
	CD4	L369P	**50**	**30**
		S375M	4	2
C4	CoR	R419A	**34**	**20**
	CoR	K421A	1	0.6
	CoR	I423A	0.43	0.3
	CD4	V430A	1	0.6
	CoR	A440E	3	1.8
C5		F468V	9	5.4
	CD4	G471E	2	1.2
	CD4	D474A	0.46	0.3
	CD4	R476A	1	0.6

[a] Amino acids were labeled based on HxB2 numbering. The residues are defined according to the designations by Kwong, Zhou, and colleagues (28, 57).
[b] The mutant IC_{50} is the concentration of the UCLA1 aptamer that inhibited 50% of infection of the respective mutant.
[c] Values representing a significant neutralization resistance are shown in bold. Values represent the average of at least three independent experiments.
[d] The fold decrease in neutralization sensitivity to the aptamer was calculated as mutant IC_{50}/wild-type IC_{50}. The wild-type IC_{50} was calculated as an average of 1.67 nM.

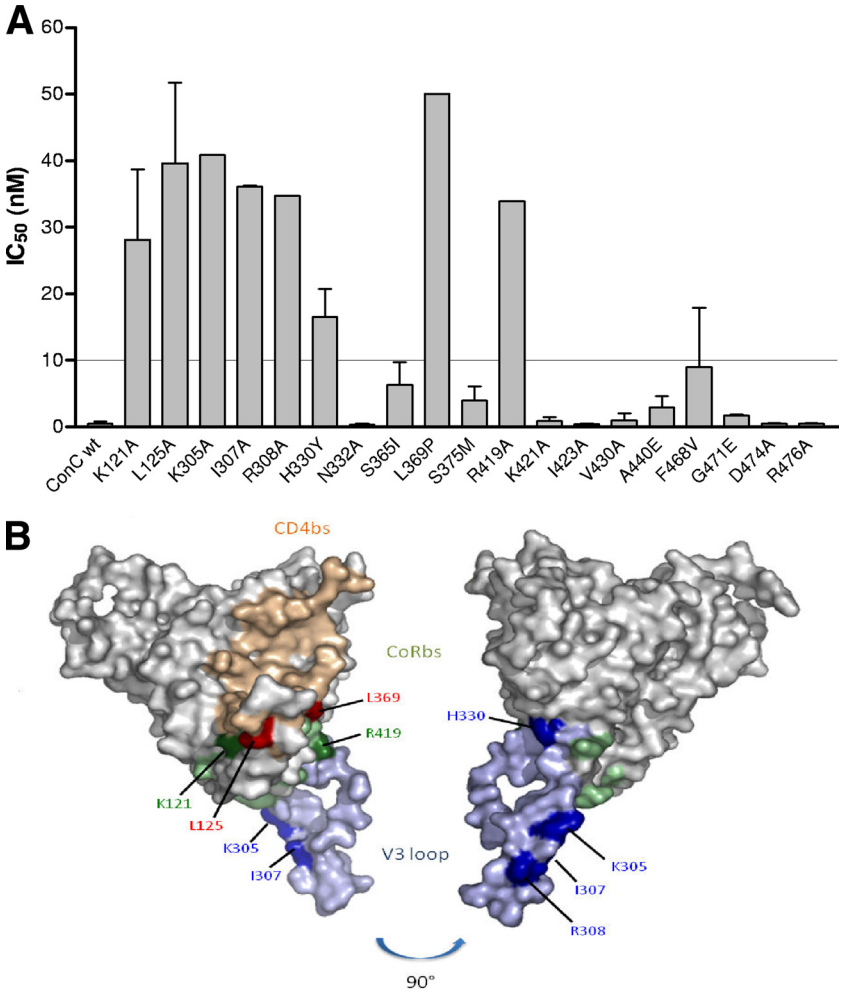

FIG 4 (A) Neutralization of ConC gp120 single-point mutants with UCLA1. Graph depicts the IC_{50}s of the mutants with those above the dotted line conferring resistance (≥10 nM). wt, wild type. (B) Structural representation of the amino acid residues involved in UCLA1 neutralization resistance. Blue depicts the V3 loop, green depicts the CoRbs, and tan depicts the CD4bs. Residues causing neutralization escape are marked in dark shades of the corresponding region. The picture was rotated at 90° for a clear view of the H330 and R308 residues. Coordinates were taken from the structure of the gp120JRFL core with V3 ligated with CD4 and X5 (Protein Data Bank accession no. 2B4C). The figure was generated with PyMOL (DeLano Scientific LLC, South San Francisco, CA [http://www.pymol.org]).

viruses (CAP84 and Du123) could not be deduced from the amino acid alignment.

A similar approach was applied to sequences from primary isolates tested for neutralization with UCLA1 in PBMCs. SW7, which was resistant in the PBMC assay, had mutations K305R, H330Y, and L369I (see Fig. S4B in the supplemental material). Since the SW7 pseudovirus contained the same changes but was sensitive in the TZM-bl assay, these residues were unlikely to be resistance conferring in the PBMC assay. Similarly, an I307V change was observed in both Du156 and Du422, which differed in their sensitivities to UCLA1 in PBMCs (see Fig. S4B). Therefore, the presence of resistance-associated mutations in some sensitive viruses in both the TZM-bl cells (see Fig. S4A) and PBMCs (see Fig. S4B) attests to the complex nature of resistance and brings into question the value of these types of analyses.

Synergy of UCLA1 with other entry inhibitors. Both T20 and b12 have been previously shown to act synergistically with other HIV-1 entry inhibitors (2, 37, 46, 58). Thus, we next evaluated any possible synergistic effects of UCLA1 with T20 or b12. Synergism

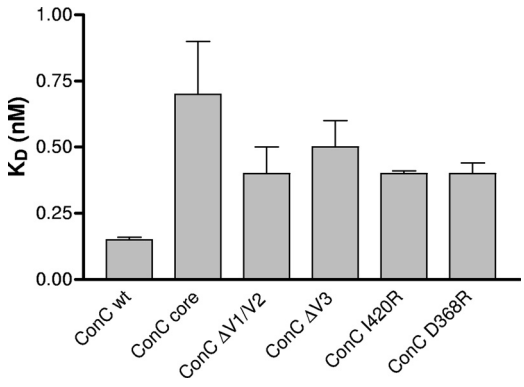

FIG 5 Bar chart representation of the K_D values of UCLA1 from the core, ΔV1/V2 and ΔV3 truncated HIV-1 ConC gp120, and from I420R (CoRbs) and D368R (CD4bs) mutated HIV-1 ConC gp120. The truncated and mutated ConC glycoproteins were compared with the K_D of the wild-type (wt) ConC gp120.

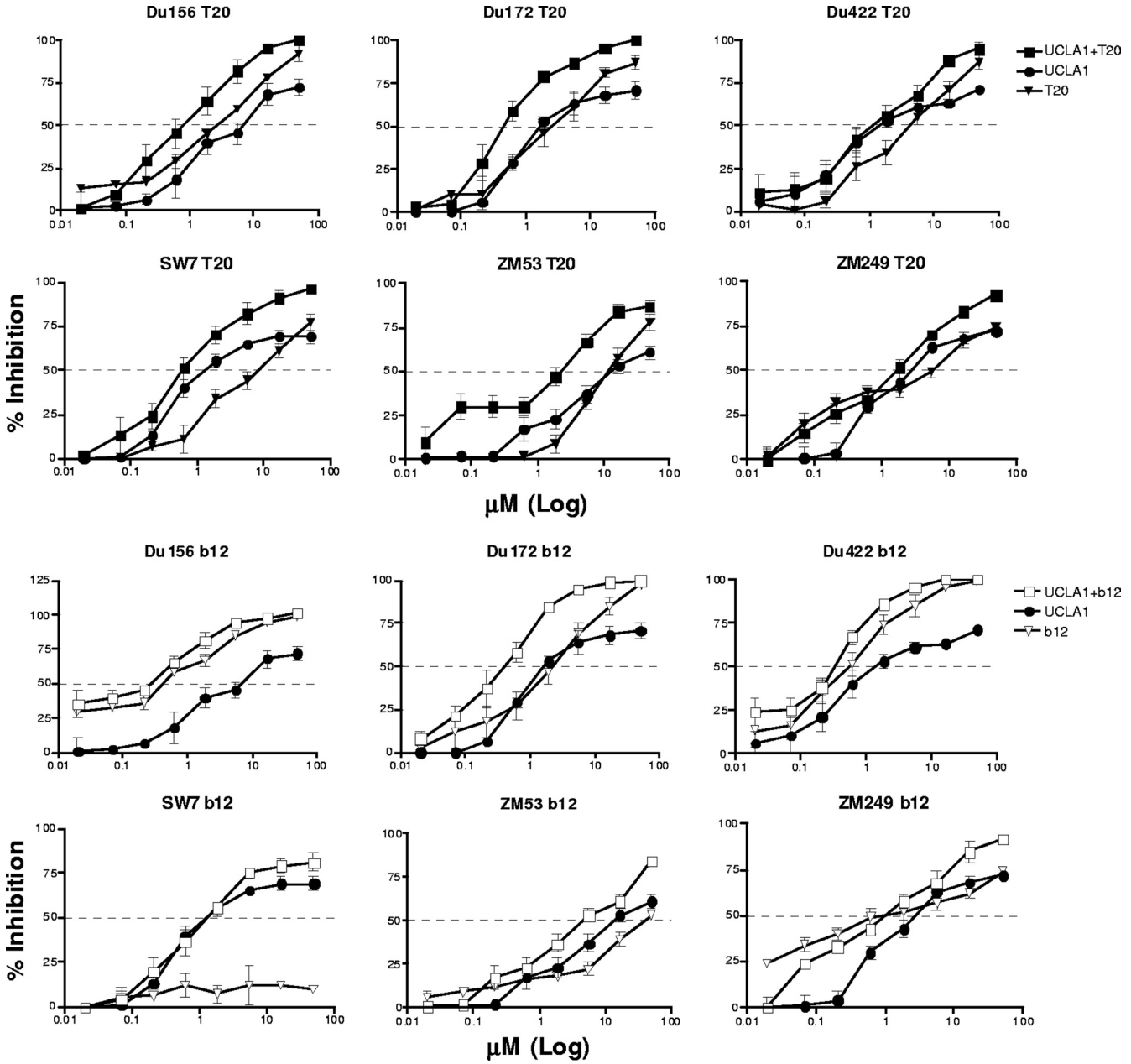

FIG 6 Dose-dependent neutralization graphs of HIV-1 subtype C Env-pseudotyped viruses showing synergism between UCLA1 and T20 or UCLA1 and b12. The aptamer was used at a maximum starting concentration of 50 nM when used alone or in combination. b12 and T20 were used at a maximum initial concentration of 50 μg/ml each and in combination with UCLA1. The 50-μg/ml concentration used for b12 and T20 is equivalent to 312 μM and 1,1131 μM, respectively.

was examined using the single-cycle neutralization assay with Env-pseudotyped viruses. The aptamer showed synergism with T20 for 5 of 6 (83%) viruses tested (Fig. 6), with CI values ranging from 0.13 to 0.46 (Table 3). Slight synergism was observed for ZM249 with UCLA1-T20, with a CI value of 0.84. There was also synergism between the aptamer and b12 MAb for 4 of 6 (67%) viruses tested (Fig. 6), with CI values ranging from 0.5 to 0.7 (Table 3). The combination of UCLA1 and b12 resulted in an additive effect (CI = 0.93) for the neutralization of Du156. Although b12 neutralization of ZM53 was relatively moderate (IC_{50} = 46.14 nM), the antibody combination with UCLA1 resulted in a 2-fold decrease of the IC_{50} (6.22 to 2.8 nM) (Table 3). There was no synergism between UCLA1 and b12 for the neutralization of SW7. This is probably due to the fact that this virus is resistant to b12 (E. Gray, unpublished data). The dose reduction indices for T20, b12, and UCLA1 were determined to be in the range of 3.7 to 27.0, 1.5 to 16.4, and 1.8 to 11.2, respectively, clearly indicating that lower concentrations of these compounds were required to neutralize the viruses, when used in combination. Thus, on average, 11-fold less T20, 5-fold less b12, and 5-fold less UCLA1 were required to neutralize virus infection when in combination.

TABLE 3 Combination therapy using the UCLA1 aptamer, T20, and b12 against subtype C Env pseudotype viruses

Virus	CI[a]	Concn of UCLA1	Concn of UCLA1 + T20 or b12	Dose reduction index[c]	Concn of T20 or b12	Concn of T20 or b12 + UCLA1	Dose reduction index[c]
		UCLA1 (nM)[b]	UCLA1 + T20 (μM)		T20 (μg/ml)[d]	T20 + UCLA1 (μM)	
Du156.12	**0.37**	1.20	0.31	3.9	2.87	0.31	9.3
Du172.17	**0.43**	1.83	0.34	5.4	1.39	0.34	4.1
Du422.1	**0.13**	3.69	0.33	11.2	8.90	0.33	27.0
SW7.14	**0.43**	0.74	0.27	2.7	3.98	0.27	14.7
ZM53 M.PB12	**0.46**	6.22	1.73	3.6	9.72	1.73	5.6
ZM249 M.PL1	0.84	2.80	1.60	1.8	5.85	1.60	3.7
		UCLA1 (nM)[b]	UCLA1 + b12 (μM)		b12 (μg/ml)[d]	b12 + UCLA1 (μM)	
Du156.12	0.93	1.20	0.30	4.0	0.44	0.30	1.5
Du172.17	**0.56**	1.83	0.22	8.3	0.50	0.22	2.3
Du422.1	**0.65**	3.69	0.53	7.0	1.04	0.53	2.0
SW7.14	1.62	0.74	1.19	0.6	50.00	1.19	42.0
ZM53 M.PB12	**0.5**	6.22	2.82	2.2	46.14	2.82	16.4
ZM249 M.PL1	**0.7**	2.80	0.87	3.2	2.26	0.87	2.6

[a] The combination index (CI) was calculated using the Chou and Talalay equation (7). CI values of 0.3 to 0.7, 0.7 to 0.85, 0.85 to 0.9, 0.9 to 1.1, and >1.1 represent synergism, moderate synergism, slight synergism, additive effect, and antagonism, respectively. CI values representing synergism are in bold.
[b] The UCLA1 aptamer was used at an initial concentration of 50 nM alone and in combination with T20 or b12.
[c] Dose reduction index is calculated as the ratio of drug concentration required for inhibition when the drug is used alone or in combination.
[d] T20 and b12 were used at an initial concentration of 50 μg/ml (equivalent to 312 μM and 11,131 μM, respectively) alone or in combination with UCLA1.

DISCUSSION

In this study, the UCLA1 RNA aptamer was examined for its antiviral activity against HIV-1 subtype C viruses. Its efficacy was demonstrated by the high binding affinity for HIV-1 ConC gp120 and broad neutralization of primary isolates and Env-pseudotyped viruses. The lack of toxicity in both TZM-bl cells and PBMCs confirmed that its action was due to its efficacy and not cell toxicity. Mapping of the aptamer binding sites revealed 8 residues that modulated neutralization resistance to the aptamer. Most of the residues were localized within the CoRbs at the base of the V3 and the bridging sheet within the conserved V1/V2 stem-loop of gp120 that makes up the CD4bs. The aptamer exhibited synergism with T20 fusion inhibitor and b12 MAb, with dose reduction indices indicating that lower concentrations of T20 and b12 can be used to inhibit HIV-1 when combined with the aptamer.

The modified UCLA1 exhibited higher affinity for its ligand compared to the parental B40 aptamer and the truncated version, B40t77 (13). The low K_D value of UCLA1 contributed to a stable association and better binding energy. This was also demonstrated by another study that showed increased binding of modified aptamers and higher potency, albeit on a limited number of viruses (10). Whether the breadth and potency of neutralization seen in our study can be attributed to UCLA1's increased affinity for gp120 requires a head-to-head comparison with other aptamers. In addition to its improved binding and its broad neutralizing activity, UCLA1 has been shown to be stable in biological fluids in a study conducted with another derivative, named UCLA005 (36). A further chemical modification (UCLA005v11) resulted in a 4-fold increase in aptamer stability with a half-life of 242 min (36), therefore confirming that modified aptamers are highly stable compounds.

UCLA1 neutralized infection of a large panel of subtype C viruses isolated from both acute and chronically infected adult and pediatric patients. There was no neutralization preference noted between viruses isolated from acute and chronic infections or between isolates from adult and pediatric patients in both the TZM-bl cells and PBMC assays. The aptamer was not strain or tropism restricted since it neutralized R5 and X4 viruses, although more X4-tropic strains need to be tested. These neutralization data concur with other studies that have utilized similar aptamers for inhibition of HIV-1 subtype B R5-tropic viruses (10, 14, 25, 36). It was noted that UCLA1 showed higher efficiency against Env-pseudotyped viruses compared to primary isolates, which has been noted by others (1, 5, 16, 30). Overall, its breadth and potency of neutralization were comparable to those of other HIV-1 entry inhibitors (1, 5, 45, 48, 49, 51). The reasons why UCLA1 was less potent in the PBMC assay are unknown but may be related to the presence of viral quasispecies, longer culture periods, nonspecific uptake by other cells, or inactivation of the aptamer in the culture. Nevertheless, high concentrations of aptamer were not cytotoxic in PBMCs. Indeed, we previously showed that the parental B40 aptamer was not toxic to PBMCs and human cardiomyocytes even at a 2 μM concentration of the aptamer (33).

Mutagenesis was performed to define the residues on gp120 influencing UCLA1 reactivity. Eight mutated residues were found to confer UCLA1 neutralization resistance. Six of these were involved in CCR5 binding and were localized at the base of the V3 loop (K305A, I307A, R308A, and H330Y), the bridging sheet within the conserved V1/V2 stem-loop that makes up the CD4-induced epitope (K121A) and the C4 domain (R419A) (28, 43, 57). Two residues in the CD4bs, K125A in the bridging sheet region and the L369P residue in the C3 domain adjacent to the Phe43 cavity (28, 40, 42), were also implicated. Residues K121, H330, L369, and R419 have been previously shown to modulate binding of other HIV-1 inhibitors within the conserved core residues (11, 40, 42, 43), including aptamers 299.5 (10) and B40t77 (23). Overall, 4 of the 8 residues were located within the V3 loop and 2 within the V1/V2 bridging sheet, confirming the SPR data using V-loop-deleted gp120 proteins, which was also shown by others (10, 14, 23, 25). Differences in the K_D values between wild-type and V-loop-deleted proteins were more subtle than the effect

of single point mutations in gp120 on neutralization. The effect of 1420R and D368R in reducing binding is likely due to their close proximity to identified residues rather than a direct effect, although this could not be tested. UCLA1 neutralization resistance could not be fully explained from the amino acid sequence alignments, probably because other residues within gp120 modulate aptamer neutralization efficacy. In addition there might be distal conformational changes that reduce UCLA1 binding affinity to gp120, as previously shown with the B40t77 aptamer against HIV-1_{BaL} gp120 (23).

Studies done by others have also shown aptamer epitopes that overlap the base of the α1 helix, the CD4-induced binding sites in the bridging sheet (β21 and β20), and the variable loops (F and V3) for 299.5 and B40t77 aptamers (10, 23). This is not surprising given that UCLA1, B40t77, and 299.5 are modified derivatives, possessing the same core structure, which is suggested to be their binding core (10, 13). We previously reported competition between B40t77 and various MAbs (23) which confirmed these mapping data. Thus, competition between B40t77 and b12 or b6 suggested shared binding sites, possibly including L369 and R419 identified in this study. Competition between B40t77 and 17b or CD4 (22) confirmed the L125 and L369 UCLA1 sites within the CD4 complex. Inhibition enhancement was observed when B40t77 was used together with the anti-V3 MAb, 19b, suggesting that the aptamer and the MAb have nonoverlapping binding sites within the V3 loop (23). This also confirms that the identified V3 loop residues are indeed UCLA1 binding sites.

UCLA1 exhibited synergism with the gp41 fusion inhibitor, T20, likely because these compounds target different regions of the viral envelope. Synergism was also noted with b12, although the effect was more modest. Since the b12 epitope includes the L369 and R419 residues, which were both shown in this study to affect UCLA1 neutralization; it was interesting to discover synergism between these two agents. This finding suggests that L369 and R419 might not be direct-contact residues for UCLA1 but peripheral sites that modulate the aptamers' reactivity accounting for the lack of competition when used in combination with b12. Alternatively, these agents might be causing an allosteric effect on the neighboring protomers, thus increasing binding affinity or site accessibility. The b12 MAb was previously shown to effectively neutralize most of the currently tested viruses (31); however, ZM53 required a higher concentration, while SW7 was resistant to this MAb (E. Gray, unpublished data). Thus, synergism between b12 and UCLA1 for ZM53 neutralization suggests that UCLA1 can increase the sensitivity of viruses that are partially resistant to the MAb. On the other hand, the lack of synergism for SW7 implies that this increase in sensitivity cannot be achieved if the virus is completely resistant to the antibody.

Taken together, the results indicate that the UCLA1 RNA aptamer has broad-spectrum potency against several subtype C viruses at low nanomolar concentrations. The noncytotoxic nature, high therapeutic index, neutralization potency, and synergistic effect of the aptamer suggest that UCLA1 can be further developed and tested in preclinical and clinical studies as a potential new entry inhibitor drug, especially against HIV-1 subtype C viruses.

ACKNOWLEDGMENTS

This work was supported by the South African Department of Science and Technology (DST) and a Council for Scientific and Industrial Research (CSIR) Parliamentary Grant. Hazel Mufhandu was funded by The Young Researcher Establishment Fund (YREF 2007 029), the Poliomyelitis Research Foundation (08/37), the Wits Medical Faculty Research Endowment Fund (001 410 MUFH011 TS), and a CSIR Ph.D. studentship. The authors acknowledge the generous donation of aptamer UCLA1 by Ian McGowan, William James, and Brian Sproat under the NIH Aptamer Microbicide Program, grant 5U01AI066734-03.

We thank Mary Phoswa (NICD), Sarah Cohen (NICD), and Lia Rotherham (CSIR) for technical assistance.

REFERENCES

1. **Alexandre KB, et al.** 2010. Mannose-rich glycosylation patterns on HIV-1 subtype C gp120 and sensitivity to the lectins, griffithsin, cyanovirin-N and scytovirin. Virology **402**:187–196.
2. **Alexandre KB, et al.** 2011. Binding of the mannose-specific lectin, griffithsin, to HIV-1 gp120 exposes the CD4-binding site. J. Virol. **85**:9039–9050.
3. **Alkhatib G, et al.** 1996. CC CKR5: a RANTES, MIP-1alpha, MIP-1beta receptor as a fusion cofactor for macrophage-tropic HIV-1. Science **272**:1955–1958.
4. **Atchison RE, et al.** 1996. Multiple extracellular elements of CCR5 and HIV-1 entry: dissociation from response to chemokines. Science **274**:1924–1926.
5. **Binley JM, et al.** 2004. Comprehensive cross-clade neutralization analysis of a panel of anti-human immunodeficiency virus type 1 monoclonal antibodies. J. Virol. **78**:13232–13252.
6. **Bures R, et al.** 2000. Immunization with recombinant canarypox vectors expressing membrane-anchored glycoprotein 120 followed by glycoprotein 160 boosting fails to generate antibodies that neutralize R5 primary isolates of human immunodeficiency virus type 1. AIDS Res. Hum. Retroviruses **16**:2019–2035.
7. **Castanotto D, Rossi JJ.** 2009. The promises and pitfalls of RNA-interference-based therapeutics. Nature **457**:426–433.
8. **Chou TC, Talalay P.** 1984. Quantitative analysis of dose-effect relationships: the combined effects of multiple drugs or enzyme inhibitors. Adv. Enzyme Regul. **22**:27–55.
9. **Cilliers T, et al.** 2003. The CCR5 and CXCR4 coreceptors are both used by human immunodeficiency virus type 1 primary isolates from subtype C. J. Virol. **77**:4449–4456.
10. **Cohen C, et al.** 2008. An aptamer that neutralizes R5 strains of HIV-1 binds to core residues of gp120 in the CCR5 binding site. Virology **381**:46–54.
11. **Cormier EG, Tran DN, Yukhayeva L, Olson WC, Dragic T.** 2001. Mapping the determinants of the CCR5 amino-terminal sulfopeptide interaction with soluble human immunodeficiency virus type 1 gp120-CD4 complexes. J. Virol. **75**:5541–5549.
12. **Decker JM, et al.** 2005. Antigenic conservation and immunogenicity of the HIV coreceptor binding site. J. Exp. Med. **201**:1407–1419.
13. **Dey AK, Griffiths C, Lea SM, James W.** 2005. Structural characterization of an anti-gp120 RNA aptamer that neutralizes R5 strains of HIV-1. RNA **11**:873–884.
14. **Dey AK, et al.** 2005. An aptamer that neutralizes R5 strains of human immunodeficiency virus type 1 blocks gp120-CCR5 interaction. J. Virol. **79**:13806–13810.
15. **Ellington AD, Szostak JW.** 1990. In vitro selection of RNA molecules that bind specific ligands. Nature **346**:818–822.
16. **Fenyo EM, et al.** 2009. International network for comparison of HIV neutralization assays: the NeutNet report. PLoS One **4**:e4505.
17. **Gray ES, Meyers T, Gray G, Montefiori DC, Morris L.** 2006. Insensitivity of paediatric HIV-1 subtype C viruses to broadly neutralising monoclonal antibodies raised against subtype B. PLoS Med. **3**:e255.
18. **Gray ES, et al.** 2007. Neutralizing antibody responses in acute human immunodeficiency virus type 1 subtype C infection. J. Virol. **81**:6187–6196.
19. **Gray ES, Moore PL, Pantophlet RA, Morris L.** 2007. N-linked glycan modifications in gp120 of human immunodeficiency virus type 1 subtype C render partial sensitivity to 2G12 antibody neutralization. J. Virol. **81**:10769–10776.
20. **Gray ES, et al.** 2009. Antibody specificities associated with neutralization breadth in plasma from human immunodeficiency virus type 1 subtype C-infected blood donors. J. Virol. **83**:8925–8937.
21. **Honnen WJ, et al.** 2007. Type-specific epitopes targeted by monoclonal antibodies with exceptionally potent neutralizing activities for selected

strains of human immunodeficiency virus type 1 map to a common region of the V2 domain of gp120 and differ only at single positions from the clade B consensus sequence. J. Virol. **81**:1424–1432.
22. **Jacobson JM, et al.** 2000. Single-dose safety, pharmacology, and antiviral activity of the human immunodeficiency virus (HIV) type 1 entry inhibitor PRO 542 in HIV-infected adults. J. Infect. Dis. **182**:326–329.
23. **Joubert MK, et al.** 2010. A modeled structure of an aptamer-gp120 complex provides insight into the mechanism of HIV-1 neutralization. Biochemistry **49**:5880–5890.
24. **Keefe AD, Pai S, Ellington A.** 2010. Aptamers as therapeutics. Nat. Rev. Drug Discov. **9**:537–550.
25. **Khati M, et al.** 2003. Neutralization of infectivity of diverse R5 clinical isolates of human immunodeficiency virus type 1 by gp120-binding 2′F-RNA aptamers. J. Virol. **77**:12692–12698.
26. **Kothe DL, et al.** 2006. Ancestral and consensus envelope immunogens for HIV-1 subtype C. Virology **352**:438–449.
27. **Kwong PD, et al.** 2002. HIV-1 evades antibody-mediated neutralization through conformational masking of receptor-binding sites. Nature **420**: 678–682.
28. **Kwong PD, et al.** 1998. Structure of an HIV gp120 envelope glycoprotein in complex with the CD4 receptor and a neutralizing human antibody. Nature **393**:648–659.
29. **Lalezari JP, et al.** 2003. Enfuvirtide, an HIV-1 fusion inhibitor, for drug-resistant HIV infection in North and South America. N. Engl. J. Med. **348**:2175–2185.
30. **Li M, et al.** 2005. Human immunodeficiency virus type 1 env clones from acute and early subtype B infections for standardized assessments of vaccine-elicited neutralizing antibodies. J. Virol. **79**:10108–10125.
31. **Li M, et al.** 2006. Genetic and neutralization properties of subtype C human immunodeficiency virus type 1 molecular env clones from acute and early heterosexually acquired infections in Southern Africa. J. Virol. **80**:11776–11790.
32. **Li Y, et al.** 2007. Broad HIV-1 neutralization mediated by CD4-binding site antibodies. Nat. Med. **13**:1032–1034.
33. **Lopes de Campos WR, Coopusamy D, Morris L, Mayosi BM, Khati M.** 2009. Cytotoxicological analysis of a gp120 binding aptamer with cross-clade human immunodeficiency virus type 1 entry inhibition properties: comparison to conventional antiretrovirals. Antimicrob. Agents Chemother. **53**:3056–3064.
34. **Montefiori DC.** 2004. Evaluating neutralizing antibodies against HIV, SIV and SHIV in luciferase reporter gene assay, **vol 12. John Wiley**, Hoboken, NJ.
35. **Moore JP, Doms RW.** 2003. The entry of entry inhibitors: a fusion of science and medicine. Proc. Natl. Acad. Sci. U. S. A. **100**:10598–10602.
36. **Moore MD, et al.** 2011. Protection of HIV neutralizing aptamers against rectal and vaginal nucleases: implications for RNA-based therapeutics. J. Biol. Chem. **286**:2526–2535.
37. **Nagashima KA, et al.** 2001. Human immunodeficiency virus type 1 entry inhibitors PRO 542 and T-20 are potently synergistic in blocking virus-cell and cell-cell fusion. J. Infect. Dis. **183**:1121–1125.
38. **O'Sullivan CK.** 2002. Aptasensors—the future of biosensing? Anal. Bioanal Chem. **372**:44–48.
39. **Osztie E, et al.** 2001. Combined intraarterial carboplatin, intraarterial etoposide phosphate, and IV cytoxan chemotherapy for progressive optic-hypothalamic gliomas in young children. AJNR Am. J. Neuroradiol. **22**: 818–823.
40. **Pantophlet R, et al.** 2003. Fine mapping of the interaction of neutralizing and nonneutralizing monoclonal antibodies with the CD4 binding site of human immunodeficiency virus type 1 gp120. J. Virol. **77**:642–658.
41. **Pinter A, et al.** 2005. The C108g epitope in the V2 domain of gp120 functions as a potent neutralization target when introduced into envelope proteins derived from human immunodeficiency virus type 1 primary isolates. J. Virol. **79**:6909–6917.
42. **Rizzuto C, Sodroski J.** 2000. Fine definition of a conserved CCR5-binding region on the human immunodeficiency virus type 1 glycoprotein 120. AIDS Res. Hum. Retroviruses **16**:741–749.
43. **Rizzuto CD, et al.** 1998. A conserved HIV gp120 glycoprotein structure involved in chemokine receptor binding. Science **280**:1949–1953.
44. **Sayer N, Ibrahim J, Turner K, Tahiri-Alaoui A, James W.** 2002. Structural characterization of a 2′F-RNA aptamer that binds a HIV-1 SU glycoprotein, gp120. Biochem. Biophys. Res. Commun. **293**:924–931.
45. **Schols D.** 2006. HIV co-receptor inhibitors as novel class of anti-HIV drugs. Antiviral Res. **71**:216–226.
46. **Tremblay CL, Kollmann C, Giguel F, Chou TC, Hirsch MS.** 2000. Strong in vitro synergy between the fusion inhibitor T-20 and the CXCR4 blocker AMD-3100. J. Acquir. Immune Defic. Syndr. **25**:99–102.
47. **Van Harmelen JH, et al.** 1999. A predominantly HIV type 1 subtype C-restricted epidemic in South African urban populations. AIDS Res. Hum. Retroviruses **15**:395–398.
48. **Walker LM, et al.** 2011. Broad neutralization coverage of HIV by multiple highly potent antibodies. Nature **477**:466–470.
49. **Walker LM, et al.** 2009. Broad and potent neutralizing antibodies from an African donor reveal a new HIV-1 vaccine target. Science **326**:285–289.
50. **Wang W, Jia L-Y.** 2009. Progress in aptamer screening methods. Chin. J. Anal. Chem. **37**:454–460.
51. **Wu X, et al.** 2010. Rational design of envelope identifies broadly neutralizing human monoclonal antibodies to HIV-1. Science **329**:856–861.
52. **Wyatt R, et al.** 1998. The antigenic structure of the HIV gp120 envelope glycoprotein. Nature **393**:705–711.
53. **Zhou J, Li H, Li S, Zaia J, Rossi JJ.** 2008. Novel dual inhibitory function aptamer-siRNA delivery system for HIV-1 therapy. Mol. Ther. **16**:1481–1489.
54. **Zhou J, Rossi JJ.** 2010. Cell-specific aptamer-mediated targeted drug delivery. Oligonucleotides **21**:1–10.
55. **Zhou J, Shu Y, Guo P, Smith DD, Rossi JJ.** 2011. Dual functional RNA nanoparticles containing phi29 motor pRNA and anti-gp120 aptamer for cell-type specific delivery and HIV-1 inhibition. Methods **54**:284–294.
56. **Zhou J, et al.** 2009. Selection, characterization and application of new RNA HIV gp 120 aptamers for facile delivery of Dicer substrate siRNAs into HIV infected cells. Nucleic Acids Res. **37**:3094–3109.
57. **Zhou T, et al.** 2007. Structural definition of a conserved neutralization epitope on HIV-1 gp120. Nature **445**:732–737.
58. **Zwick MB, et al.** 2005. Anti-human immunodeficiency virus type 1 (HIV-1) antibodies 2F5 and 4E10 require surprisingly few crucial residues in the membrane-proximal external region of glycoprotein gp41 to neutralize HIV-1. J. Virol. **79**:1252–1261.
59. **Zwick MB, et al.** 2001. Neutralization synergy of human immunodeficiency virus type 1 primary isolates by cocktails of broadly neutralizing antibodies. J. Virol. **75**:12198–12208.